JSER

Performance Prediction of Conventional and Modified Solar Stills Using Levenberg Marquardt Algorithm-Based Artificial Neural Network Model: An Experimental and Stochastic Evaluation

Rishika Chauhan[a,*], Shefali Sharma[a], Rahul Pachauri[b]

[a]*Department of Electronics and Communication Engineering, Jaypee University of Engineering and Technology, A.B. Road, Raghogarh-473226, Guna, Madhya Pradesh, India.*
[b]*Department of Computer Science and Engineering, Jaypee University of Engineering and Technology, A.B. Road, Raghogarh-473226, Guna, Madhya Pradesh, India.*

ARTICLE INFO

A B S T R A C T

A neural network (ANN) model employing the Levenberg-Marquardt (LM) algorithm was formulated and employed to study the functionality of both conventional (CSS) and modified (MSSW and MSSU) solar distillation systems. Numerous input factors, comprising solar irradiance, wind speed, atmospheric conditions, glass properties, and water temperatures, were carefully selected, with the yield of distilled water serving as the target variable. The model underwent a process of testing, training, and validation utilizing empirical data obtained from CSS, MSSW, and MSSU setups, achieving a confidence level of 95%. After validation, the model's capabilities were utilized to forecast the distilled water output based on a distinct set of input parameters. The outcomes unveiled a negligible deviation, with a maximum disparity of 3.1% and 4.6% observed in comparison to the experimental findings for MSSW, and MSSU setups, respectively, thereby signifying a substantial agreement between theoretical predictions and experimental observations. Furthermore, the model exhibited outstanding accuracy in contrast to well-established numerical models proposed by several researchers, thereby demonstrating its efficacy in predicting the performance of solar stills.

1. Introduction

Water, an indispensable element, critical for everyone's survival, is facing increasing pollution, largely attributed to human activities, particularly which everyone's existence rely are disappearing, and the worldwide yearly per person accessibility of drinkable water is diminishing while the demand is steadily rising. This crisis is not limited to

*Corresponding Author Email:rishikaster@gmail.com

developing nations; even developed countries are grappling with a potable water shortage [1,2].

Addressing this pressing issue, especially in impoverished regions with burgeoning populations, necessitates earnest efforts to cultivate sustainable, environmental friendly, and inexpensive machinery or techniques for changing brackish or saline water into drinkable water [3–6]. Among these solutions, the conventional solar still (CSS) stands out as devices utilizing solar energy to facilitate the conversion process. However, their efficacy is hindered by low productivity and a substantial requirement for surface area [7–11].

To boost the effectiveness of solar stills, scientists are actively investigating three key factors: the temperature of the glass, water temperature, and the surface area of the water. By raising the temperature of the water and expanding the evaporation area while simultaneously decreasing the temperature of the condensing cover, substantial improvements in still productivity can be achieved. Researchers are actively exploring improvements in these areas to improve the efficiency of CSS [12–15].

Sodha et al. [16] explored the operation of a multi-wick solar still, which resulted in a largest collective output of 2.45 kg/m^2 under sunlight. Jamil and Akhtar [17] explored the characteristic height, specifically aspect ratios ranging from 1.94 to 2.67, on the CSS yield. Dumka and Mishra [18] have investigated the influence of salinity strength on the heat transfer coefficient of a solar distiller. The collective efforts of researchers aim to overcome the limitations of distillers and significantly enhance their productivity for a green solution to the global potable water crisis. Velmurugan et al. [19] explored enhancements to CSS by introducing fins and sponges, resulting in a significant yield increase of 40.2% and 45%, respectively. Dhivagar et al. [20] have reported the integration of black powder-coated crushed granite stone with solar desalination and district heating to enhance both water production and cooling efficiency of solar desalination unit. The impact of magnetic power (which will act as energy storage medium) of the performance of solar distiller unit has been experimentally explored by Dhivagar et al. [21].

Deshmukh and Thombre [22] explored the integration of sand and "servo-therm medium oil" as an energy storing substance underneath the baseliner of a CSS. Khanafer and Vafai [23] conducted an extensive examination of the use of nanofluids in CSS. Dumka and Mishra [24,25] conducted an in-depth relative assessment of enhanced solar still (combined with the earth) and a CSS. In an experimental study, Kabeel et al. [26] presented a relative analysis of 3 diverse solar distiller units: CSS, CSS enhanced with energy storage, and CSS enhanced with jute-knitted energy storage, by examining variations in water in basin. These research endeavours offer valuable perspectives for enhancing the efficiency and efficacy of solar stills, tackling the hurdles linked with potable water generation.

Alaian et al. [27] took out experimental studies on CSS enhanced with "pin-finned wicks". Their conclusions indicated a remarkable improvement in performance and yield of wick-augmented and pin-finned CSS, with increments of 23% and 55%, respectively, when compared to a standard CSS. These studies contribute valuable insights into innovative modifications to solar still designs, offering increased efficiency and higher distillate yields for sustainable water production. Alamshah et al. [28] have reported an experimental study where they have used a 3-D solar distiller unit to study the impact of shape on the performance of solar distiller units. Shoeibi et al. [29] have reported an extensive review on the performance of solar energy systems in the presence of PCM. In another study Hemmatian et al. [30] have mentioned the use of PCM on heat pipes and solar collectors.

Kumar et al. [31] have documented the augmentation of honeycomb in CSS to increase its distillate due to the waters capillary action. Dumka et al. [32] have communicated the application of Plexiglas and wick to increase the performance of CSS due to the capillary effect and heat localization. To meet the demand for precise and dependable modelling of solar energy systems [33–38], researchers have turned to Artificial Neural Network (ANN) models as a viable alternate to conventional approaches [39–45]. The successful application of ANN models in this context is attributed to their capability to handle the substantial uncertainty inherent in solar energy data. Extensive studies have established ANN as a robust tool for modelling various engineering systems [46–49]. Dumka et al. [50] have reported the use of saltwater bottles in the CSS cavity to improve the energy holding capacity of still. Due to the presence of Saltwater bottles, they have recorded an improvement of 25.4% in the distillate yield.

Dumka et al. [51] utilized ANN to project the yield of CSS enhanced with jute-covered balls. Mashaly and Alazba [52] constructed a model based on ANN which aimed at forecasting the yield, efficiency, and effective recovery ratio of a solar

distillation unit. Their findings underscored the precision and efficiency of the model in projecting the behaviour of the still with minimal errors. Chauhan et al. [53] demonstrated that how one can estimate the moist air properties by using ANN. Their study unveiled that LM algorithm is the best to predict the properties.

Previous research has primarily focused on two approaches: Improving water temperature and surface area through the application of latent and sensible energy storage materials, while lowering condensing cover temperature by circulating water across it. To increase surface area, Dumka and Mishra [54] proposed an ultrasonic fogger within the CSS basin. However, they found that while the fogger performed well during sunny hours, its effectiveness decreased substantially in the evening due to excessive fogging. To address this issue, Dumka et al. [55] incorporated a cotton cloth envelope, acting as a tent to absorb excess mist created by the fogger while also reducing the characteristic length of the solar stills. However, they noted the complexity of developing a mathematical model for such arrangements and minimized theoretical analysis accordingly.

In this article, the authors address the problem by developing an ANN model to simulate the complex physics of a CSS, both with and without the integration of an ultrasonic fogger and cotton cloth. The experiments were conducted multiple times to refine the ANN-based theoretical model, which evaluates the performance of the CSS and its variations: CSS with a fogger and wick (MSSW) and CSS with an ultrasonic fogger (MSSU), specifically in predicting distillate output.

The key novelties of this work include the development and implementation of an Artificial Neural Network (ANN) model, specifically using the Levenberg-Marquardt (LM) algorithm, to predict the performance of various solar distillation systems accurately (CSS, MSSW, and MSSU). This approach allows for a unified evaluation of multiple input factors such as solar irradiance, wind speed, atmospheric conditions, and water temperatures. Moreover, the model's ability to forecast distilled water output with a high degree of precision (less than 5% deviation) and its noteworthy improvement over traditional numerical methods (as proposed by Dunkle [56], Kumar & Tiwari [57], and Tsilingiris [58,59]) in predicting the yield. The model not only make easy the evaluation of solar still performance but also go beyond the complexity of existing heat and mass transfer analyses. Additionally, the ANN model's validation using experimental data from multiple solar distillation setups is another novel contribution, offering a robust and reliable method for future predictions in solar distillation research. These advancements show a meaningful contribution to the field, by providing a more accurate and efficient predictive tool for assessing solar still performance.

2. Experimental setup

Three identical single-slope conventional solar stills, facing south, were constructed using 5 mm thick FRP material. The stills featured lower and higher vertical edge heights measuring 19.5 and 64.5 cm, respectively. To optimize the absorption of incident solar radiations, both stills were internally coated with black paint. Bubble wrap was employed to stop the energy dissipation from the below and sides of the stills. The basin water was contained in blackened Galvanized iron trays, having a thickness of 0.74 mm, occupying 1 m^2 area and standing at a height of 10 cm within both stills. For top coverage, 4 mm broad glass were utilized, forming 24° angle with the ground, reflecting the latitudinal site of Guna, India. This construction aimed to create an efficient CSS setup while considering the geographical context.

In one still, an ultrasonic fogger (MSSW) is placed, while in another, both cotton cloth and fogger are utilized (MSSW). The third setup is kept unchanged for comparison (CSS).

An ultrasonic fogger operates using a piezoelectric ceramic disc that is powered by current through two nickel electrodes. The piezoelectric nature of the ceramic causes it to oscillate at an ultrasonic frequency when an electric current is applied, making the sound waves in the water silent. As the oscillation frequency of plate increases, the water attempts to follow but, due to its weight and inertia, cannot keep up, resulting in a phenomenon known as water hammering [60,61]. This mismatch between the water's motion and the oscillating plate creates a low-pressure area between them, which causes the formation of a cavity, a process known as cavitation. When the cavity collapses, it releases a significant amount of energy, producing a powerful imploding jet. Simultaneously, the vibrating disc generates capillary waves, or ripples, on the water's surface due to Taylor instability [62]. These capillary waves continue oscillating because of gravity and surface tension. When the cavity collapses, it creates a cross-patterned wave on the water surface, and tiny droplets at the wave crests break free from the surface tension. These droplets

are then carried away by the air above the water, emerging from the humidifier as mist. The size of the droplets becomes smaller as the oscillation frequency increases. If the capillary waves oscillate at approximately half of the driving frequency, the atomization threshold tends to be proportional to the viscosity of the water [60,63].

As the solar radiation decreases after the evening time, mist formation inside the solar still increases (as radian intensity decreases to zero), leading to a reduced evaporation rate. To address the issue of excessive misting and improve overall yield, Dumka and Mishra [55] have proposed the use of a cotton cloth mounted on a metallic frame, placed over the basin area. This setup acts as a shelter, covering both the basin water and the fogger. Thus, reducing the chances of mist to come in direct contact of the inner condensing cover.

The stills were analysed using 50 kg water in it, as suggested by Dumka and Mishra [54]. Temperature measurements were conducted using thermocouples of type K (model K 7/32-2C-TEF), while radiation intensity of sun rays was obtained using a solar-power-meter (model LX-107). The collection of the distillate was done using Borosil measuring flasks. The FlikFinz Mist Maker (B07GTWWQ4N) fogger is utilized during the experiment. The Photographs of CSS, MSSU, and MSSW are presented in Fig.1.

Standard uncertainties (u) of Type B are judged [64–68] which are evaluated as: $a/\sqrt{3}$ where, a is the device accuracy. The value of u for thermocouple, graduated cylinder, and solar power meter came out as 0.06°C, 0.6 ml, and 5.77 W/m^2 for an accuracy of ±0.1°C, ±1 ml, and ±10 W/m^2, respectively.

Fig. 1. Photographs of Solar Stills

3. Method

3.1. ANN architecture

Neural networks draw inspiration from the human brain, enabling them to mimic human-like thinking patterns. These networks, commonly known as ANN (artificial neural networks), are constructed using artificial neurons as their basic components. Within an ANN model, weights (denoted as w) play a crucial role in establishing connections between multiple neurons [69,70]. These neurons operate in parallel, receiving weighted input data through incoming connections, as illustrated in Fig. 2. The network output is generated by summing up these inputs and subjecting them to an activation function (like sigmoid, ReLU, or tanh). This function determines the output of the neuron by introducing non-linearity. The final output can be sent to other neurons or produce a final result. Through careful adjustment of weights (w) and bias (b), neurons can adapt for various forms of generalization. This adjustment process, known as training, refines the network's performance [71].
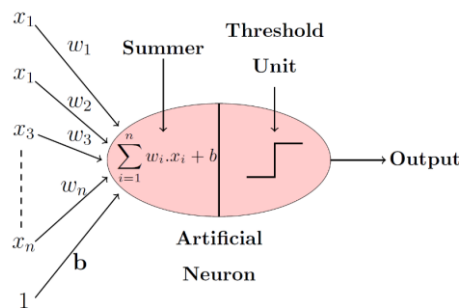

Fig. 2. Artificial neuron

ANN is generally characterized into networks of "feedback" and "feedforward" characteristics. The data flows unidirectionally commencing at the input neuron to the output neuron in a feedforward ANN. These networks can be either simple, suitable for addressing straightforward problems, or multi-layered, adept at handling complex problems. In a multi-layered neural network, the yield of one layer acts as subsequent layers input, often involving several hidden layers [72]. Kalogirou and Bojic [40] proposed a formula (Eq. 1) to get the quantity of hidden nodes (M) in a hidden layer based on input and output nodes count.

$$M = (input\ neurons + output\ neurons)/2 + \sqrt{(Number\ of\ training\ data)}$$

(1)

The backpropagation algorithm (BP) is employed to train these multilayer ANNs, wherein the error function is minimized using the gradient descent technique. Through error function backpropagation, adjustments are made to the network weights [72].

3.2. LM algorithm

This algorithm is a variant of Backpropagation method (BP), employs both Gauss-Newton & steepest descent techniques to minimize the error-function, rendering it a hybrid algorithm [73–75]. A notable advantage of this algorithm is its power to accomplish second-order training pace without requiring evaluation of the H (Hessian matrix). Consequently, weight adjustments are made efficiently when utilizing LM algorithm. Unlike methods with a constant step size, LM algorithm dynamically adjusts the step size throughout iterations, initially starting with a large value and progressively decreasing it as the task advances. This step size variation is attributed to the combination of steepest descent and Gauss-Newton techniques [76].

In the BP algorithm, the MSE (mean square error) is adopted as the indicator of performance, and its gradient (g) and Hessian matrix (H) approximation are represented with the help of network error vector (e) and Jacobian matrix (J) as follows [72,77]:

$$g = J^T e \qquad (2)$$

$$H = J^T J \qquad (3)$$

In the LM algorithm, the Hessian matrix approximation is computed in the Newton-update step as follows [53]:

$$x_{k+1} = x_k - (J^T J + \mu I)^{-1} J^T e \qquad (4)$$

where, I is the identity matrix. For a large value of step size (μ), LM algorithm behaves akin to gradient descent, while for lesser values, it resembles Gauss-Newton. By combining the strengths of "Gauss-Newton" and gradient descent approaches, the LM algorithm effectively addresses the given problem.

3.3. Evaluation parameters

Several statistical parameters are used to access the efficacy of LM algorithm, such as: overall model performance index (OI), root mean square error ($RMSE$), coefficient of residual mass (CRM), and efficiency coefficient (EC). $RMSE$ acts as a gauge of the precision of forecasts generated by the ANN model. A lower $RMSE$ value indicates more accurate predictions. EC and OI assess the fitness between actual and predicted data. Both EC and OI have maximum values of 1, indicating an accurate match between predicted and observed data. Therefore, the closer EC and OI are to 1, the better the match.

CRM provides insight into whether the model overestimates or underestimates data relative to its true value. Ideally, CRM should approach zero for a perfect match between observed and forecasted values. The numerical expressions for these statistical parameters are as follows [40,42,69,72–74,78]:

$$RMSE = \sqrt{\frac{\sum_{i=1}^{n}(a_{p,i}-a_{o,i})^2}{n}} \qquad (5)$$

$$EC = 1 - \frac{\sum_{i=1}^{n}(a_{p,i}-a_{o,i})^2}{\sum_{i=1}^{n}(a_{p,i}-\bar{a}_o)^2} \qquad (6)$$

$$OI = \frac{1}{2}\left(1 - \frac{RMSE}{a_{max}-a_{min}} + E\right) \qquad (7)$$

$$CRM = \frac{\sum_{i=1}^{n}a_{p,i}-\sum_{i=1}^{n}a_{o,i}}{\sum_{i=1}^{n}a_{o,i}} \qquad (8)$$

where, $a_{p,i}$, $a_{o,i}$, n, a_{max}, a_{min} are the predicted value, observed value, number of samples, maximum observed value, minimum observed value.

3.4. ANN methodology adopted

In this research paper, a feedforward, BP, ANN, with three layers has been employed, comprising one input, one hidden, and one output layers. For model training, LM algorithm was utilized. Five variables, namely T_w (water temperature), T_{ci} (glass temperature), I' (solar intensity), T_a (atmospheric temperature), and v_{wind} (wind velocity) serve as input variables for the neurons in the input layer for CSS, MSSU, and MSSW. For modified solar still with fogger and wick (MSSW), two more variables are included as input, wick_in and wick_out. The neuron in the output layer is connected to the yield ($\dot{m}_{ew}$). An artificial neural network with neuron numbers (12, 1) was constructed, indicating 12 hidden layer neurons and one output layer neuron as shown in Fig. 3. MATLAB 2020 was utilized for training, testing, and validating the designed network model.
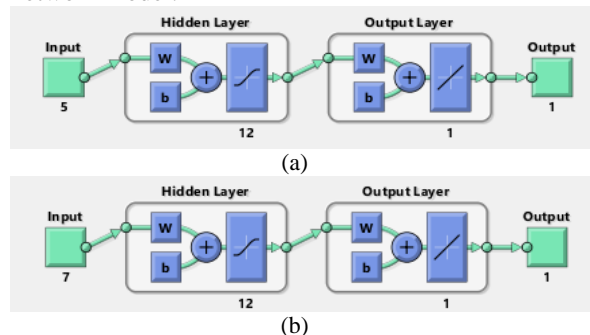

(a)

(b)

Fig. 3. ANN model used (a) CSS and MSSU (b) MSSW

The following were the assumptions used in the analysis:

- The properties of the materials used (such as the glass and the construction of the solar still) remain consistent during the experiments and model predictions.
- The solar irradiance is measured at the same intervals and is uniformly distributed across the surface of the solar stills.
- The wind speed, air temperature, and humidity are assumed to be stable during the testing periods.
- The insulation of the solar stills is perfect, or negligible heat loss occurs through the sides or bottom of the setup.
- The systems (CSS, MSSW, and MSSU) are assumed to have reached steady-state operation.
- The water used in the solar stills is assumed to have consistent salinity levels.
- The empirical data used for training, testing, and validating the ANN model are assumed to be representative of typical operational conditions for the solar distillation systems.
- The ANN model is assumed to provide accurate predictions based on the specific input parameters.
- The environmental factors not included in the model, such as dust on the glass or minor air flow variations.

4. Results and Discussion

The dataset in use is segmented into three subsets for training, validation, and testing. During the teaching phase, gradients/Jacobians are processed utilizing the training set, with weight adjustments executed after every iteration. Simultaneously, the validation set is employed to monitor the performance of ANN between training instances, evaluating the associated validation error. If, across multiple iterations, the validation error starts to rise, the training process is ceased, and the weights corresponding to the lowest error are chosen as the ultimate weights for trained network.

The strewn points on the validation error-graph indicate instances of improved validation error. Ultimately, the efficacy of the trained model is assessed using the test data.
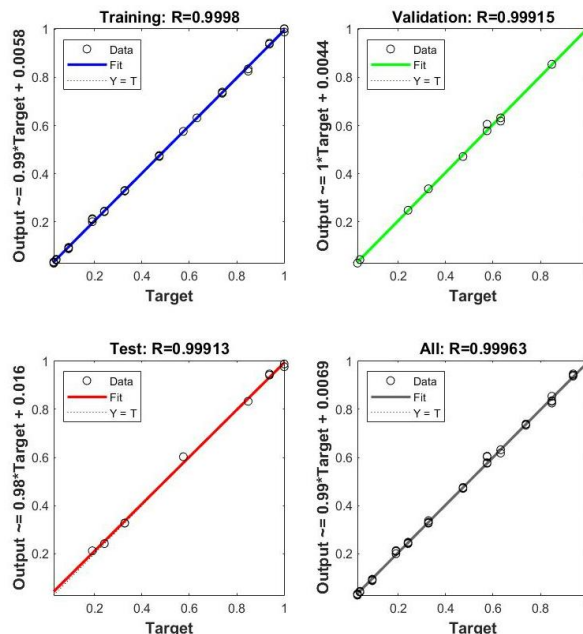

Fig.4. Regression plot for CSS

In Fig. 4, regression plots depict the relationship relating the network and the actual outputs. Throughout the stages of training, validation, and testing, the correlation coefficients stand at 0.9998, 0.9992, and 0.9991, respectively for CSS. This indicates a close correspondence between the predicted and actual outputs, i.e., it can predict outputs with high accuracy. The overall correlation coefficient averages at 0.9996, underscoring the precision of the model's forecasts relative to the true values. The minor circles represent the data points, while the dashed line indicates situation where the acquired results match the targeted values. The continuous line depicts the optimal fitting among the predicted and the aimed values. A high correlation coefficient usually implies that the model has learned the underlying patterns in the data very well.
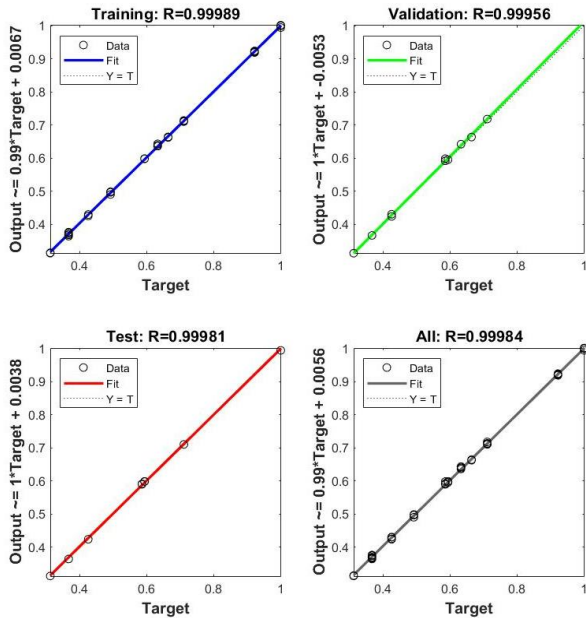
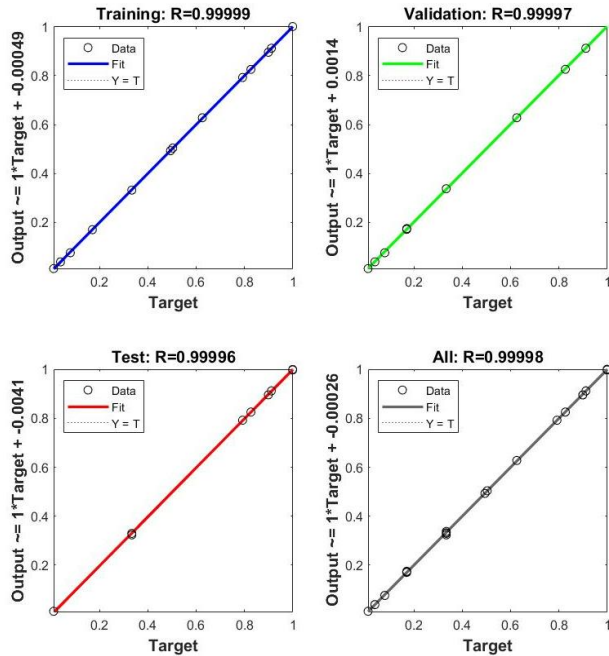Fig. 5. Regression plot for MSSW

Fig. 6. Regression plot for MSSU

Fig. 5 and 6 represent the training, testing, and validation correlation coefficients for the overall data for MSSW and MSSU. The values obtained from the designed ANN model are 0.9999, 0.9996, and 0.9998 for MSSW and 0.9999, 0.9999, and 0.9999 for MSSU respectively. These values indicate that the predicted outputs closely follow the actual outputs.

The overall correlation coefficients are 0.9998 and 0.9999 for MSSW and MSSU respectively, highlighting the strong relationship between the predicted and actual values.
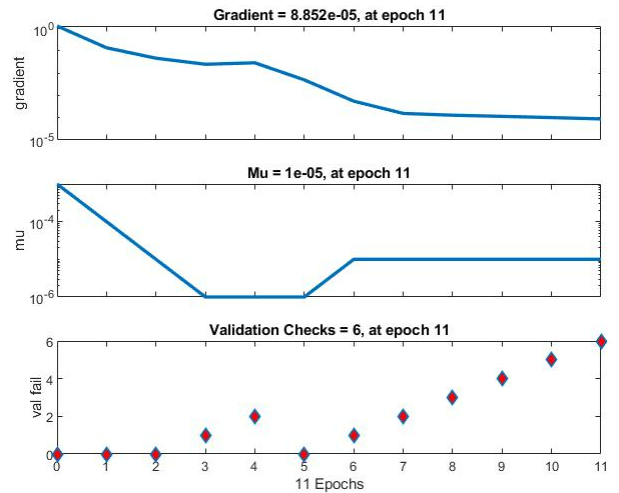

Fig. 7. Training state for CSS

Fig. 7 highlights the deviation in gradient error, validation checks, and adjustments in step size for CSS. Gradient refers to the derivative of the loss function with respect to the model parameters. It indicates the direction and rate of change for model optimization. Gradient Error arises when there is a discrepancy or noise in the calculated gradient, potentially due to insufficient data, noisy samples, or other factors. Validation Checks refer to periodic evaluations performed during training to monitor the model's performance on the validation set. It helps in detecting whether the model is improving or if early stopping is needed to avoid overfitting. Step size determines how big of a step the algorithm should take in the direction of the gradient during each update to the model's parameters. It controls the speed and precision of parameter updates during training. In Fig. 7, the detected gradient error is 8.852×10^{-5} at the 11th epoch. The gradient error is relatively small, showing the model is likely making more accurate updates to its parameters, which is a good indication of stable training. The validation checks and step size are 6 and 10^{-6}, correspondingly, i.e., after every 6 epochs, the model's performance is checked against the validation dataset and the model is making very small, gradual updates to its parameters during training, which can help ensure precision and stability in learning. The gradient error of 0.00015849 and 1.4408×10^{-9} for MSSW and MSSU are noted with validation checks at 6 and 4 respectively as displayed by the Fig. 8 and 9.
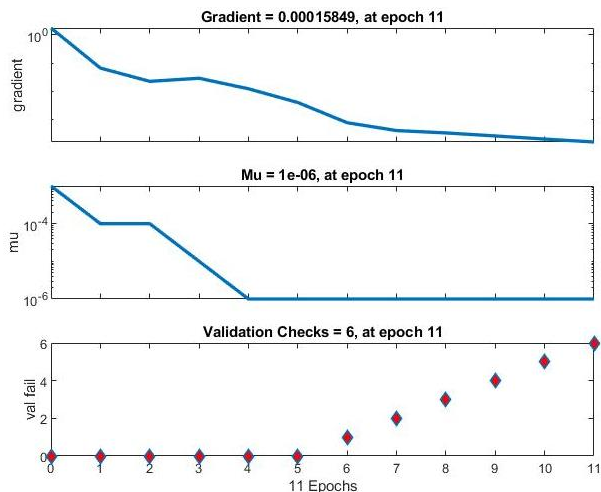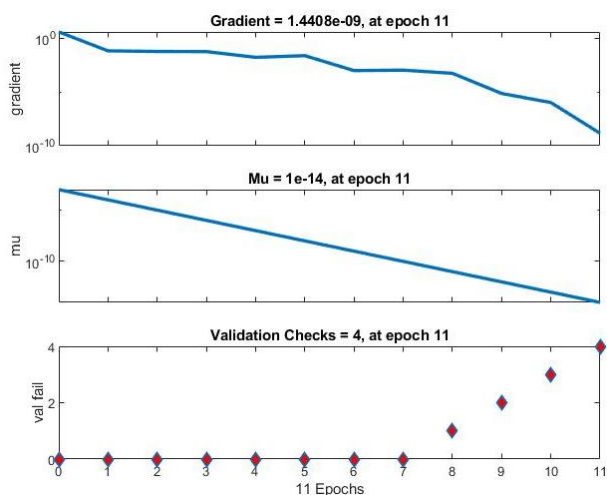
Fig. 8. Training state for MSSW

Fig. 9. Training state for MSSU

Fig. 10. Variation of MSE performance for CSS
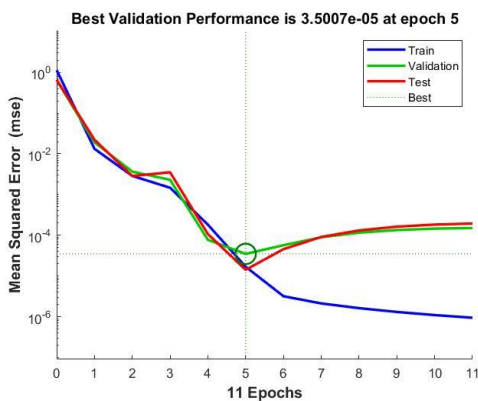
Fig. 11. Variation of MSE performance for MSSW
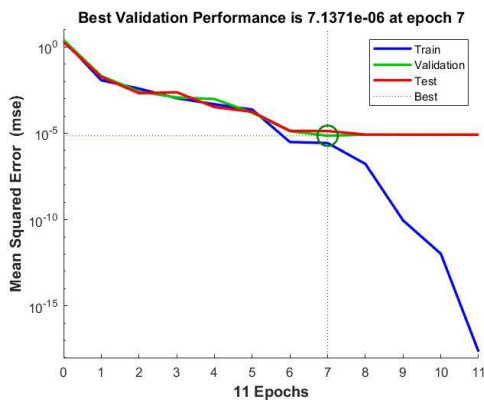
Fig. 12. Variation of MSE performance for MSSU

Figs. 10, 11 and 12 exhibit the mean square error performance of CSS, MSSW and MSSU at epoch 11 as 0.000134, 3.5×10^{-5} and 7.137×10^{-6}, respectively. As lower MSE indicates better performance, MSSU outperforms both MSSW and CSS, as it has the lowest mean square error, indicating its predictions are closest to the actual values. CSS performs the worst with the highest MSE, and MSSW falls in between but is closer to MSSU in terms of performance.
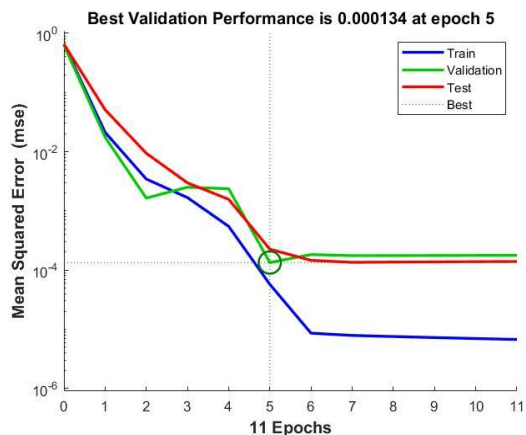
Table 1. Observed values of RMSE, EC, OI and CRM

	CSS	MSSW	MSSU
RMSE	0.0135	0.0061	0.0031
EC	0.9991	0.9995	1
OI	0.9926	0.9953	0.9984
CRM	0.0040	0.0037	-5.8×10^{-4}

Table 1 displays the RMSE, CRM, OI, and EC and values acquired by the developed ANN model, demonstrating its optimal alignment between network output and real output through the LM algorithm. The suggested model exhibits a robust fit, accurately predicting actual outputs, as evidenced by the proximity of RMSE and CRM values to zero and the closeness of EC and OI values to one. All three systems are predicted accurately by the ANN model, but MSSU shows the highest level of precision and reliability.

The suggested model provides a simple way to predict yields from CSS, MSSW, and MSSU without needing advanced knowledge of heat and mass transfer. By using straightforward input variables, the model calculates performance parameters like RMSE, EC, OI, etc. which makes it easy to apply in various contexts.

Utilizing input parameters from CSS, MSSW and MSSU experiments, the recommended ANN model has been employed to forecast distillate output. Fig. 13 illustrates the % error deviation for the three stills given by suggested ANN model.
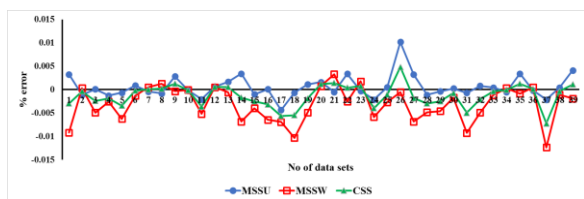

Fig. 13. % error variation of ANN based on the concerned data set

These results prove the efficiency of the ANN in precisely forecasting the results as the theoretical heat and mass transfer models (Dunkle [56], Kumar & Tiwari [79], and Tsilingiris [59,80]) predicts the distillate which deviates much more than the experimental results [54,55].

5. Conclusions

Drawing from the acquired experimental results and the recommended ANN model, following conclusions are derived:

- Understanding the input factors facilitates the straightforward evaluation of CSS, MSSW, and MSSU performance employing the suggested ANN model.

- The training process for the CSS, MSSW, and MSSU models demonstrates stable and precise optimization, as indicated by the small gradient errors and controlled updates to the model parameters, minimizing overfitting and ensuring reliable model performance.

- The precision of the suggested ANN model can be readily assessed by analyzing various metrics such as CRM, RMSE, OI, EC, and R^2 obtained for CSS, MSSW, and MSSU. MSSU demonstrates the best performance, with the lowest prediction error (RMSE $=0.0031$), perfect efficiency (EC $=1$), and minimal bias (CRM $= -5.8 \times 10^{-4}$), making it the most accurate system predicted by the ANN model. MSSW performs better than CSS across all metrics, showing greater accuracy and less bias. CSS performs adequately but has slightly higher prediction errors compared to MSSU and MSSW.

- The anticipated yield for CSS, MSSU, and MSSW shows less than 5% variance compared to their respective experimental counterparts. It shows that the proposed ANN model can be trusted to make accurate yield forecasts with minimal error, making it a valuable tool for practical applications.

- The designed model is particularly advantageous for predicting the future yield of MSSW and MSSU, outperforming complex heat and mass transfer analyses reported by several researchers [41,42].

Future work will focus on expanding the current ANN model by including additional environmental and operational parameters, such as varying water salinity levels, different geographic locations, and seasonal variations, to further improve its predictive abilities. Additionally, efforts will be made to integrate real-time data acquisition systems into the model, enabling dynamic performance forecasting of solar distillation systems under changing environmental conditions. Finally, additional comparison with other machine learning algorithms will be explored to assess whether alternative

models can offer improvements in predictive accuracy and computational efficiency.

Nomenclature	
a	Accuracy of instrument
$a_{p,i}$	predicted value
$a_{p,o}$	observed value
a_{max}	maximum predicted value
a_{min}	minimum predicted value
b	bias
e	error vector
g	gradient
H	Hessian matrix
$I(t)$	incident solar radiation on inclined cover surface (W/m^2)
I	identity matrix
J	Jacobian matrix
J^T	transpose of Jacobian matrix
m_{ew}	distillate yield (ml)
n	number of samples
R	correlation coefficient
R^2	coefficient of determination
T_a	ambient temperature
T_{ci}	inner glass cover temperature
T_w	temperature of water surface
u	standard uncertainty
w_i	weight
x_i	input variable
Greek Letter	
μ	step size
Abbreviations	
ANN	artificial neural network
BP	Back propagation
CSS	conventional solar still
CRM	coefficient of residual mass
LM	Levenberg Marquardt
EC	Efficiency coefficient
MSSU	modified solar still integrated with ultrasonic fogger
MSSW	modified solar still integrated with wick
MSE	Mean square error
OI	overall index of model performance
RMSE	root mean square error

References

[1] WWC, World Water Council Report - 8th World water forum highlights, 2018. http://www.worldwatercouncil.org/sites/default/files/2018-11/Outcomes-of-8th-WWForum_WEB.pdf.

[2] REN21, Renewables 2015-Global status report, 2015. https://doi.org/10.1016/0267-3649(88)90030-1.

[3] M.S.H. Boutilier, J. Lee, V. Chambers, V. Venkatesh, R. Karnik, Water filtration using plant xylem., PLoS One 9 (2014) e89934. https://doi.org/10.1371/journal.pone.0089934.

[4] A. Ahmad, T. Azam, Water Purification Technologies, in: A.M. Grumezescu, A.M. Holban (Eds.), Bottled Packag. Water, Woodhead Publishing, 2019: pp. 83–120. https://doi.org/https://doi.org/10.1016/B978-0-12-815272-0.00004-0.

[5] G.N. Tiwari, A. Tiwari, Shyam, Solar Distillation, Pergamon, Oxford, U.K, UK, 2016. https://doi.org/10.1007/978-981-10-0807-8_13.

[6] G.N. Tiwari, A.K. Tiwari, Solar Distillation Practice for Water Desalination Systems, Anamaya, New Delhi, India, 2008.

[7] K. Zarzoum, K. Zhani, H. Ben Bacha, Desalination and Water Treatment, 126 (2018) 87–96. https://doi.org/10.5004/dwt.2018.22812.

[8] H.M. Yeh, L.C. Chen, The effects of climatic, design and operational parameters on the performance of wick-type solar distillers, Energy Convers. Manag. 26 (1986) 175–180. https://doi.org/10.1016/0196-8904(86)90052-X.

[9] H. Panchal, Solar Desalination Technology Brief, in: A. Kumar, O. Prakash (Eds.), Sol. Desalin. Technol., Springer Singapore, 2019: pp. 167–177. https://doi.org/10.1007/978-981-13-6887-5.

[10] B.W. Tleimat, E.D. Howe, Nocturnal production of solar distillers, Sol. Energy 10 (1966) 61–66. https://doi.org/10.1016/0038-092X(66)90037-5.

[11] A.A. El-Sebaii, E. El-Bialy, Advanced designs of solar desalination systems: A review, Renew. Sustain. Energy Rev. (2015). https://doi.org/10.1016/j.rser.2015.04.161.

[12] P. Prakash, V. Velmurugan, Parameters influencing the productivity of solar stills – A review, Renew. Sustain. Energy Rev. 49 (2015) 585–609. https://doi.org/10.1016/j.rser.2015.04.136.

[13] S. Shoeibi, N. Rahbar, A. Abedini Esfahlani, H. Kargarsharifabad, A review of techniques for simultaneous enhancement of evaporation and condensation rates in solar stills, Sol. Energy 225 (2021) 666–693.

https://doi.org/10.1016/j.solener.2021.07.02
8.

[14] K. Selvaraj, A. Natarajan, Factors in fl
uencing the performance and productivity of
solar stills - A review, Desalination 435
(2018) 181–187.
https://doi.org/10.1016/j.desal.2017.09.031.

[15] M.S. Barghi Jahromi, V. Kalantar, H.
Samimi Akhijahani, H. Kargarsharifabad, S.
Shoeibi, Performance analysis of a new solar
air ventilator with phase change material:
Numerical simulation, techno-economic and
environmental analysis, J. Energy Storage
62 (2023) 106961.
https://doi.org/10.1016/j.est.2023.106961.

[16] M.S. Sodha, A. Kumar, G.N. Tiwari, R.C.
Tyagi, Simple multiple wick solar still:
Analysis and performance, Sol. Energy 26
(1981) 127–131.
https://doi.org/10.1016/0038-
092X(81)90075-X.

[17] B. Jamil, N. Akhtar, Effect of specific height
on the performance of a single slope solar
still: An experimental study, Desalination
414 (2017) 73–88.
https://doi.org/10.1016/j.desal.2017.03.036.

[18] P. Dumka, D.R. Mishra, Influence of salt
concentration on the performance
characteristics of passive solar still, Int. J.
Ambient Energy 42 (2021) 1463–1473.
https://doi.org/10.1080/01430750.2019.1611
638.

[19] V. Velmurugan, C.K. Deenadayalan, H.
Vinod, K. Srithar, Desalination of effluent
using fin type solar still, Energy 33 (2008)
1719–1727.
https://doi.org/10.1016/j.energy.2008.07.001
.

[20] R. Dhivagar, S. Shoeibi, H.
Kargarsharifabad, M. Sadi, A. Arabkoohsar,
M. Khiadani, Performance analysis of solar
desalination using crushed granite stone as
an energy storage material and the
integration of solar district heating, Energy
Sources, Part A Recover. Util. Environ. Eff.
46 (2024) 1370–1388.
https://doi.org/10.1080/15567036.2023.2299
693.

[21] R. Dhivagar, S. Shoeibi, H.
Kargarsharifabad, M.H. Ahmadi, M.
Sharifpur, Performance enhancement of a
solar still using magnetic powder as an
energy storage medium-exergy and
environmental analysis, Energy Sci. Eng. 10

(2022) 3154–3166.
https://doi.org/10.1002/ese3.1210.

[22] H.S. Deshmukh, S.B. Thombre, Solar
distillation with single basin solar still using
sensible heat storage materials, Desalination
410 (2017) 91–98.
https://doi.org/10.1016/j.desal.2017.01.030.

[23] K. Khanafer, K. Vafai, A review on the
applications of nanofluids in solar energy
field, Renew. Energy 123 (2018) 398–406.
https://doi.org/10.1016/j.renene.2018.01.097
.

[24] P. Dumka, D.R. Mishra, Energy and exergy
analysis of conventional and modified solar
still integrated with sand bed earth: Study of
heat and mass transfer, Desalination 437
(2018) 15–25.
https://doi.org/10.1016/j.desal.2018.02.026.

[25] P. Dumka, D.R. Mishra, Experimental
investigation of modified single slope solar
still integrated with earth (I) &(II):Energy
and exergy analysis, Energy 160 (2018)
1144–1157.
https://doi.org/10.1016/j.energy.2018.07.083
.

[26] A.E. Kabeel, S.A. El-agouz, R.
Sathyamurthy, T. Arunkumar, Augmenting
the productivity of solar still using jute cloth
knitted with sand heat energy storage,
Desalination 443 (2018) 122–129.
https://doi.org/10.1016/j.desal.2018.05.026.

[27] W.M. Alaian, E.A. Elnegiry, A.M. Hamed,
Experimental investigation on the
performance of solar still augmented with
pin-finned wick, Desalination 379 (2016)
10–15.
https://doi.org/10.1016/j.desal.2015.10.010.

[28] S.A. Alamshah, M. Talebzadegan, M.
Moravej, Performance Evaluation of
Regular Hexagonal Pyramid Three-
Dimensional Solar Desalination System : An
Experimental Investigation, J. Sol. Energy
Res. 9 (2024) 1914–1925.
https://doi.org/10.22059/jser.2024.370071.1
371.

[29] S. Shoeibi, F. Jamil, S.M. Parsa, S. Mehdi,
H. Kargarsharifabad, S.A.A. Mirjalily, W.
Guo, H.H. Ngo, B.J. Ni, M. Khiadani,
Recent advancements in applications of
encapsulated phase change materials for
solar energy systems: A state of the art
review, J. Energy Storage 94 (2024) 112401.
https://doi.org/10.1016/j.est.2024.112401.

[30] A. Hemmatian, H. Kargarsharifabad, A.

Abedini Esfahlani, N. Rahbar, S. Shoeibi, Improving solar still performance with heat pipe/pulsating heat pipe evacuated tube solar collectors and PCM: An experimental and environmental analysis, Sol. Energy 269 (2024) 112371. https://doi.org/10.1016/j.solener.2024.112371.

[31] R. Kumar, D.R. Mishra, P. Dumka, Improving solar still performance : A comparative analysis of conventional and honeycomb pad augmented solar stills, Sol. Energy 270 (2024) 112408. https://doi.org/https://doi.org/10.1016/j.solener.2024.112408.

[32] P. Dumka, D.R. Mishra, B. Singh, R. Chauhan, M. Haque, I. Siddiqui, Enhancing solar still performance with Plexiglas and jute cloth additions : experimental study, Sustain. Environ. Res. 34 (2024) 2–12. https://doi.org/10.1186/s42834-024-00208-y.

[33] N. Hashemian, A. Noorpoor, Assessment and multi-criteria optimization of a solar and biomass-based multi-generation system: Thermodynamic, exergoeconomic and exergoenvironmental aspects, Energy Convers. Manag. 195 (2019) 788–797. https://doi.org/10.1016/j.enconman.2019.05.039.

[34] N. Hashemian, A. Noorpoor, Thermo-eco-environmental Investigation of a Newly Developed Solar/wind Powered Multi-Generation Plant with Hydrogen and Ammonia Production Options, J. Sol. Energy Res. 8 (2023) 1728–1737. https://doi.org/10.22059/jser.2024.374028.1388.

[35] M.S. Barghi Jahromi, V. Kalantar, H. Samimi Akhijahani, H. Kargarsharifabad, Recent progress on solar cabinet dryers for agricultural products equipped with energy storage using phase change materials, J. Energy Storage 51 (2022) 104434. https://doi.org/10.1016/j.est.2022.104434.

[36] Z. Younsi, H. Naji, A numerical investigation of melting phase change process via the enthalpy-porosity approach: Application to hydrated salts, Int. Commun. Heat Mass Transf. 86 (2017) 12–24. https://doi.org/https://doi.org/10.1016/j.icheatmasstransfer.2017.05.012.

[37] M.P.R. Teles, M. Sadi, K.A.R. Ismail, A. Arabkoohsar, B.V.F. Silva, H. Kargarsharifabad, S. Shoeibi, Cooling supply with a new type of evacuated solar collectors: a techno-economic optimization and analysis, Environ. Sci. Pollut. Res. 31 (2024) 18171–18187. https://doi.org/10.1007/s11356-023-25715-0.

[38] Y. Cao, H. Nikafshan Rad, D. Hamedi Jamali, N. Hashemian, A. Ghasemi, A novel multi-objective spiral optimization algorithm for an innovative solar/biomass-based multi-generation energy system: 3E analyses, and optimization algorithms comparison, Energy Convers. Manag. 219 (2020) 112961. https://doi.org/https://doi.org/10.1016/j.enconman.2020.112961.

[39] F.A. Essa, M. Abd Elaziz, A.H. Elsheikh, An enhanced productivity prediction model of active solar still using artificial neural network and Harris Hawks optimizer, Appl. Therm. Eng. 170 (2020) 115020. https://doi.org/10.1016/j.applthermaleng.2020.115020.

[40] S.A. Kalogirou, M. Bojic, Artificial neural networks for the prediction of the energy consumption of a passive solar building, Energy 25 (2000) 479–491. https://doi.org/10.1016/S0360-5442(99)00086-9.

[41] S.A. Kalogirou, E. Mathioulakis, V. Belessiotis, Arti fi cial neural networks for the performance prediction of large solar systems, Renew. Energy 63 (2014) 90–97. https://doi.org/10.1016/j.renene.2013.08.049.

[42] A. Katal, N. Singh, Artificial Neural Network: Models, Applications, and Challenges, in: R. Tomar, M.D. Hina, R. Zitouni, A. Ramdane-Cherif (Eds.), Innov. Trends Comput. Intell., Springer International Publishing, Cham, 2022: pp. 235–257. https://doi.org/10.1007/978-3-030-78284-9_11.

[43] A.F. Mashaly, A.A. Alazba, Thermal performance analysis of an inclined passive solar still using agricultural drainage water and artificial neural network in arid climate, Sol. Energy 153 (2017) 383–395. https://doi.org/10.1016/j.solener.2017.05.083.

[44] J. Jawad, A.H. Hawari, S. Javaid Zaidi, Artificial neural network modeling of wastewater treatment and desalination using membrane processes: A review, Chem. Eng.

J. 419 (2021) 129540. https://doi.org/https://doi.org/10.1016/j.cej.2021.129540.

[45] E. Najafi, R. Rajabi, N. Bayat, Fault Tolerant Multilevel Inverter Using Artificial Neural Network, J. Sol. Energy Res. 9 (2024) 1745–1752. https://doi.org/10.22059/jser.2024.359461.1309.

[46] A.H. Elsheikh, S.W. Sharshir, M. Abd Elaziz, A.E. Kabeel, W. Guilan, Z. Haiou, Modeling of solar energy systems using artificial neural network: A comprehensive review, Sol. Energy 180 (2019) 622–639. https://doi.org/10.1016/j.solener.2019.01.037.

[47] A. Bardossy, L. Duckstein, Fuzzy Rule-Based Modeling with Applications to Geophysical, Biological and Engineering Systems, CRC press, 2022. https://doi.org/10.1201/9780138755133.

[48] R.P. Chen, P. Zhang, X. Kang, Z.Q. Zhong, Y. Liu, H.N. Wu, Prediction of maximum surface settlement caused by earth pressure balance (EPB) shield tunneling with ANN methods, Soils Found. 59 (2019) 284–295. https://doi.org/10.1016/j.sandf.2018.11.005.

[49] K.S. Garud, S. Jayaraj, M.Y. Lee, A review on modeling of solar photovoltaic systems using artificial neural networks, fuzzy logic, genetic algorithm and hybrid models, Int. J. Energy Res. 45 (2021) 6–35. https://doi.org/10.1002/er.5608.

[50] P. Dumka, N. Pandey, D.R. Mishra, Conventional Solar Still Augmented with Saltwater Bottles: An Experimental Study, J. Sol. Energy Res. 9 (2024) 1811–1821. https://doi.org/10.22059/jser.2024.374131.1392.

[51] P. Dumka, R. Chauhan, D.R. Mishra, Experimental and theoretical evaluation of a conventional solar still augmented with jute covered plastic balls, J. Energy Storage 32 (2020) 101874. https://doi.org/10.1016/j.est.2020.101874.

[52] A.F. Mashaly, A.A. Alazba, Neural network approach for predicting solar still production using agricultural drainage as a feedwater source, Desalin. Water Treat. 57 (2016) 28646–28660. https://doi.org/10.1080/19443994.2016.1193770.

[53] R. Chauhan, S. Sharma, R. Pachauri, P. Dumka, D.R. Mishra, Experimental and theoretical evaluation of thermophysical properties for moist air within solar still by using different algorithms of artificial neural network, J. Energy Storage 30 (2020) 101408. https://doi.org/10.1016/J.EST.2020.101408.

[54] P. Dumka, D.R. Mishra, Performance evaluation of single slope solar still augmented with the ultrasonic fogger, Energy 190 (2020) 116398. https://doi.org/10.1016/j.energy.2019.116398.

[55] P. Dumka, A. Jain, D.R. Mishra, Energy, exergy, and economic analysis of single slope conventional solar still augmented with an ultrasonic fogger and a cotton cloth, J. Energy Storage 30 (2020). https://doi.org/10.1016/j.est.2020.101541.

[56] R.V. Dunkle, Solar water distillation: the roof type still and a multiple effect diffusion still, in: Int. Dev. Heat Transf. ASME, Proc. Int. Heat Transf. Part V, Univ. Color., 1961: pp. 895–902.

[57] S. Kumar, G.N. Tiwari, Estimation of convective mass transfer in solar distillation systems, Sol. Energy 57 (1996) 459–464. https://doi.org/10.1016/S0038-092X(96)00122-3.

[58] P.T. Tsilingiris, Modeling heat and mass transport phenomena at higher temperatures in solar distillation systems – The Chilton – Colburn analogy, Sol. Energy 84 (2010) 308–317. https://doi.org/10.1016/j.solener.2009.11.012.

[59] P.T. Tsilingiris, Parameters affecting the accuracy of Dunkle ' s model of mass transfer phenomenon at elevated temperatures, Appl. Therm. Eng. 75 (2015) 203–212. https://doi.org/10.1016/j.applthermaleng.2014.09.010.

[60] B. Avvaru, M.N. Patil, P.R. Gogate, A.B. Pandit, Ultrasonic atomization: Effect of liquid phase properties, Ultrasonics 44 (2006) 146–158. https://doi.org/10.1016/j.ultras.2005.09.003.

[61] A.J. Yule, Y. Al-Suleimani, On droplet formation from capillary waves on a vibrating surface, Proc. R. Soc. A Math. Phys. Eng. Sci. 456 (2000) 1069–1085. https://doi.org/10.1098/rspa.2000.0551.

[62] G.I. Taylor, The instability of liquid surfaces when accelerated in a direction

perpendicular to their planes. I, in: Proc. R. Soc. London. Ser. A. Math. Phys. Sci., 1950: pp. 192–196. https://doi.org/10.1098/rspa.1950.0052.

[63] J.D. Bassett, A.W. Bright, Observations concerning the mechanism of atomisation in an ultrasonic fountain, J. Aerosol Sci. 7 (1976) 47–51. https://doi.org/10.1016/0021-8502(76)90008-2.

[64] J.P. Holman, Experimental methods for engineers, McGraw-Hill, New York, 2017.

[65] P. Dumka, K. Gajula, K. Sharma, D.R. Mishra, R. Chauhan, M.I. Haque Siddiqui, D. Dobrotă, I.M. Rotaru, A case study on single basin solar still augmented with wax filled metallic cylinders, Case Stud. Therm. Eng. 61 (2024) 104847. https://doi.org/10.1016/j.csite.2024.104847.

[66] B. Khalili, H. Kargarsharifabad, N. Rahbar, A. Abedini Esfahlani, E. Jamshidi, Performance evaluation of a CGS gas heater-powered HDH desalination system using thermosyphon heat pipes: An experimental study with economic and environmental assessment, Int. Commun. Heat Mass Transf. 152 (2024) 107300. https://doi.org/https://doi.org/10.1016/j.icheatmasstransfer.2024.107300.

[67] B. Omidi, N. Rahbar, H. Kargarsharifabad, Z. Poolaei Moziraji, Performance evaluation of a solar desalination-hot water system using heat pipe vacuum tube parabolic trough solar collector – An experimental study with Taguchi analysis, Energy Convers. Manag. 292 (2023) 117347. https://doi.org/https://doi.org/10.1016/j.enconman.2023.117347.

[68] R. Dhivagar, S. Shoeibi, S.M. Parsa, S. Hoseinzadeh, H. Kargarsharifabad, M. Khiadani, Performance evaluation of solar still using energy storage biomaterial with porous surface: An experimental study and environmental analysis, Renew. Energy 206 (2023) 879–889. https://doi.org/10.1016/j.renene.2023.02.097.

[69] P. Gao, L. Zhang, K. Cheng, H. Zhang, W. Yaïci, E. Entchev, A. Qazi, H. Fayaz, A. Wadi, R.G. Raj, N.A. Rahim, W.A. Khan, The artificial neural network for solar radiation prediction and designing solar systems: A systematic literature review, J. Clean. Prod. 104 (2014) 1348–1359. https://doi.org/10.1016/j.jclepro.2015.04.041

[70] T. Ertekin, Q. Sun, Artificial neural network applications in reservoir engineering, Artif. Neural Networks Chem. Eng. (2017) 123–204. https://doi.org/10.3390/en12152897.

[71] S.C. Kothari, H. Oh, Neural Networks for Pattern Recognition, Oxford University Press, 1993. https://doi.org/10.1016/S0065-2458(08)60404-0.

[72] M.T. Hagan, H.B. Demuth, M. Beale, Neural network design, PWS Publishing Co., 1997.

[73] R. Chauhan, P. Dumka, D.R. Mishra, Modelling conventional and solar earth still by using the LM algorithm-based artificial neural network, Int. J. Ambient Energy 43 (2022) 1389–1396. https://doi.org/10.1080/01430750.2019.1707113.

[74] K. Hidouria, D.R. Mishra, A. Benhmidenea, B. Chouachia, Modelling conventional and solar earth still by using the LM algorithm-based artificial neural network, IEEE Commun. Surv. Tutorials 21 (2020) 1–5. https://doi.org/10.1016/j.est.2020.101408.

[75] R. Chauhan, S. Sharma, R. Pachauri, Deep Neural Network-Based Prediction of the COVID-19 Spread in India, 3 (2021) 1–11. https://doi.org/http://doi.org/10.5281/zenodo.4574861.

[76] J. Gao, Y. Zhang, Y. Du, Q. Li, Optimization of the tire ice traction using combined Levenberg–Marquardt (LM) algorithm and neural network, J. Brazilian Soc. Mech. Sci. Eng. 41 (2019) 40. https://doi.org/10.1007/s40430-018-1545-2.

[77] F.E. Jalal, Y. Xu, M. Iqbal, M.F. Javed, B. Jamhiri, Predictive modeling of swell-strength of expansive soils using artificial intelligence approaches: ANN, ANFIS and GEP, J. Environ. Manage. 289 (2021) 112420. https://doi.org/10.1016/j.jenvman.2021.112420.

[78] J.R. Rabuñal, J. Dorado, Artificial neural networks in real-life applications, 2005. https://doi.org/10.4018/978-1-59140-902-1.

[79] S. Aggarwal, G.N. Tiwari, Thermal modelling of a double condensing chamber solar still: An experimental validation, Energy Convers. Manag. 40 (1999) 97–114. https://doi.org/10.1016/S0196-8904(98)00110-1.

[80] P.T. Tsilingiris, ScienceDirect Theoretical

derivation and comparative evaluation of mass transfer coefficient modeling in solar distillation systems – The Bowens ratio approach, Sol. ENERGY 112 (2015) 218–231. https://doi.org/10.1016/j.solener.2014.11.021.